Electronic Supplementary Material (ESI) for Environmental Science: Nano.

Supplementary material

Precisely controlling and predicting nitrogen release rate of urea-formaldehyde nanocomposite fertilizer for efficient nutrient management

Yang Xiang[a], Xudong Ru[b], Yaqing Liu[a,*], Rui Miao[a], Yingfang Tong[a], Mingshan Gong[a], Yuhan Liu[a], Guizhe Zhao[a,*]

[a]*Shanxi Province Key Laboratory of Functional Nanocomposites, Research Center for Engineering Technology of Polymeric Composites of Shanxi Province, and College of Materials Science and Engineering, North University of China, Taiyuan 030051, China*

[b]*School of Artificial Intelligence, Beijing Normal University, Beijing,100875, China*

*Corresponding Author

E-mail addresses: lyq@nuc.edu.cn (Y.Q. Liu), zgz@nuc.edu.cn (G.Z. Zhao).

Table S1. Basic physicochemical properties of the soil used in the pot study.

Soil properties	Value
Sand (%)	38
Silt (%)	50
Clay (%)	12
pH(1:2.5, soil: water)	7.87
CEC(cmol kg^{-1})	14.73
OM(g kg^{-1})	16.76
total N(g kg^{-1})	0.61
AP(mg kg^{-1})	31.47
AK(mg kg^{-1})	65.33

Table S2. Basic characteristics of the two fertilizers.

characteristics	UF+MKP	UF/MKP
carbon content (%)	17.1	16.7
nitrogen content (%)	22.5	21.3
phosphorus (P_2O_5) content (%)	22.5	21.0
potassium (K_2O) content (%)	14.9	13.9

Table S3. Fertilization formulas of the three treatments.

Treatment	Mass of fertilizers mixed directly with the soil(g)	Mass of fertilizers loaded into each net bag (g)
CK	\	\
UF+MKP	33.42	1.67
UF/MKP	35.26	1.76

Table S4. Cumulative N release rates (%) of UF/MKP with different MKP contents cultivated in soil.

Time (day)	UF	UF/MKP-0.06	UF/MKP-0.12	UF/MKP-0.18	UF/MKP-0.24	UF/MKP-0.48
1	18.37	17.02	15.62	14.62	12.55	9.49
3	21.26	20.63	19.27	18.27	17.00	15.27
5	23.66	23.27	22.96	22.30	21.77	20.56
7	25.37	25.27	24.68	25.30	24.99	24.25
10	26.64	26.96	27.07	27.22	27.61	27.27
14	28.65	29.35	30.27	30.30	30.66	31.06
21	29.97	31.53	32.95	34.28	35.60	36.60
28	31.56	33.63	35.70	37.66	38.60	40.45
42	33.04	35.65	38.70	40.66	42.66	47.69
56	34.04	36.86	40.15	43.27	47.85	56.66
70	34.64	37.65	41.52	45.66	51.52	62.86
84	35.23	38.27	42.36	47.66	54.58	67.25
98	35.72	38.65	43.23	49.85	56.95	70.62

Table S5. Predicted N release rate of UF/MKP at different tomato growth periods based on neural network model and the total deviation between predicted N release rate and tomato fertilizer requirement under different MKP content.

Samples	Predicted N release rate (%)			Total deviation (%)[a]
	0-40 days	40-70 days	70-100 days	
UF/MKP25	43.88	6.70	3.29	53.89
UF/MKP30	44.82	9.44	4.68	50.70
UF/MKP35	46.06	11.87	5.82	48.37
UF/MKP40	47.31	14.14	6.00	47.17
UF/MKP45	48.56	15.15	7.41	46.00
UF/MKP50	49.77	15.18	9.84	44.75
UF/MKP55	51.11	15.09	11.18	44.84
UF/MKP60	52.86	14.58	13.43	44.85
UF/MKP65	55.20	13.49	15.15	46.56
UF/MKP70	57.80	12.19	15.10	50.51
UF/MKP75	60.07	11.46	14.80	53.81

[a] $Total\ deviation = \sum |q_t - Q_t|$

Here, q_t and Q_t denoted predicted N release rate and tomatoes need fertilizer rate at different tomato growth periods, respectively.

Table S6. Total weight and number of tomato fruits collected at different times.

Treatment / Index / Date	CK		UF+MKP		UF/MKP	
	Total weight (g)	NO.	Total weight (g)	NO.	Total weight (g)	NO.
2017.8.1	0.00	0	0	0	47.45	5
2017.8.8	0.00	0	51.06	6	85.43	11

2017.8.15	32.36	9	92.42	11	122.65	15
2017.8.22	0.00	0	303.84	36	371.84	44
2017.8.28	233.14	45	258.00	28	355.06	46
Total	265.50	54	705.32	81	982.43	121

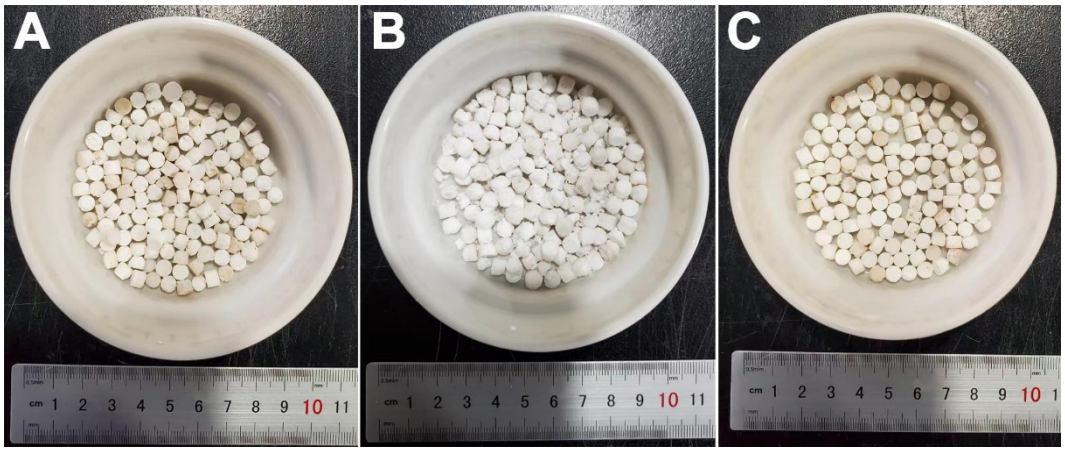

Fig. S1. Digital photos of UF (A), UF+MKP (B), and UF/MKP (C).

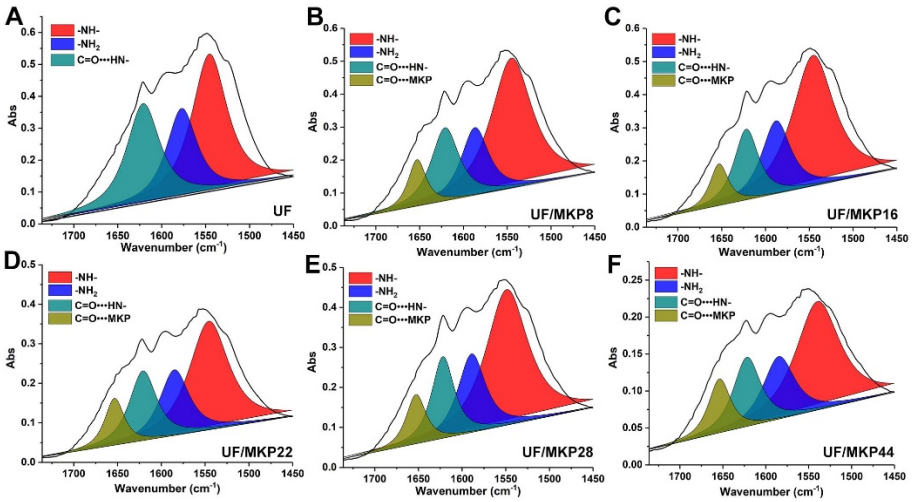

Fig. S2. Curve fitting of FTIR spectra of UF/MKP with different MKP contents in the regions of 1450-1736 cm^{-1}.

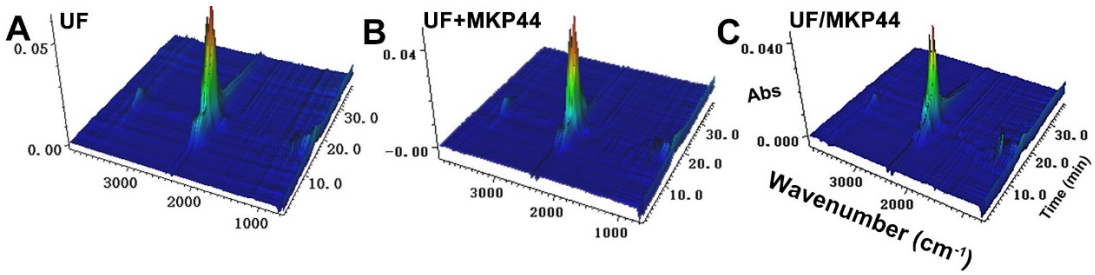

Fig. S3. 3D FTIR spectra of the gaseous products of UF, UF+MKP44 and UF/MKP44.

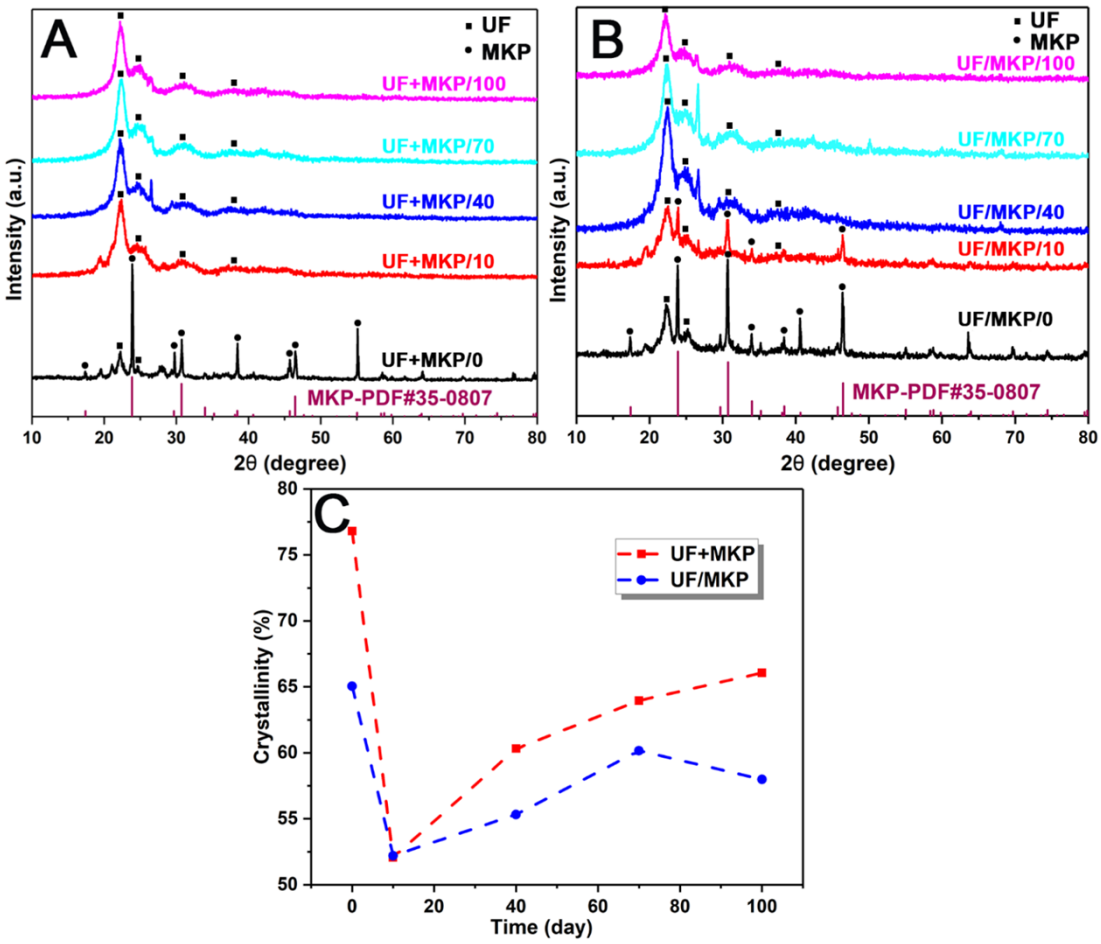

Fig. S4. XRD patterns of UF+MKP (A) and UF/MKP (B) at different soil culture periods and the degree of crystallinity of the two composites as a function of degradation time (C).

In order to accurately distinguish the UF+MKP and UF/MKP samples obtained during different tomato cultivation periods, we used UF+MKP/m and UF/MKP/m to represent them, where m indicated the number of days when the samples were taken. XRD was employed to evaluate changes in the crystalline structures of UF+MKP and UF/MKP during degradation processes. Furthermore, MDI jade software was used to fit the XRD curve to analyze the changes in the crystallinity of the fertilizers quantitatively, and the results are shown in **Fig. S4**. As shown in **Fig. S4A** and **S4B**, the diffraction peaks of MKP in the spectrum of UF+MKP/10 completely disappear after 10 days of culture, while those still exist in the UF/MKP/10 spectrum. In addition, characteristic peaks at 2θ = 22.4°, 24.8°, 31.1°, and 37.4° visually confirm the existence of distinct crystalline regions in the UF matrix. In **Fig. S4C**, the

crystallinity of UF+MKP/10 and UF/MKP/10 decrease obviously after 10 days of cultures, owing to the rapid release of MKP crystals. Afterward, the crystallinity of the simple physical mixing system UF+MKP gradually increases, indicating that the degradation occurs primarily in the amorphous regions of UF. However, the crystallinity of UF/MKP exhibits an increase followed by a reduction, indicating that significant degradation occurs even in the crystalline regions of UF after a period of cultivation in the soil, which causes a decrease in crystallinity. All these results again indicate that the interaction mode between MKP and UF significantly affects the degradation pattern and degradation rate of the UF matrix.

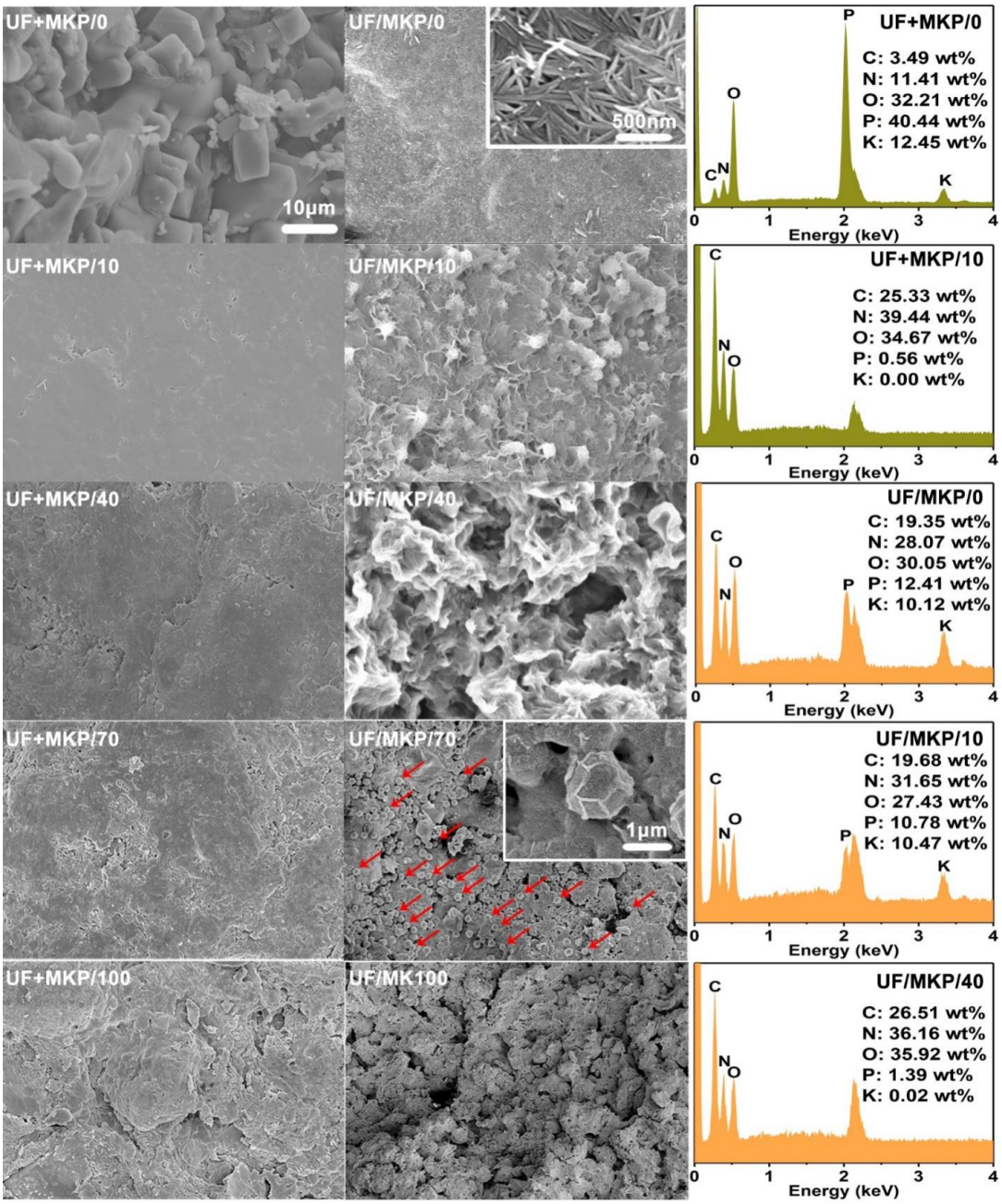

Fig. S5. SEM images and EDX spectra of UF+MKP and UF/MKP at different soil culture periods. Scales in the unmarked SEM images are exactly the same as that in UF+MKP/0.

The morphology and element content changes of UF+MKP and UF/MKP during degradation process can be clearly observed by SEM and EDX, as shown in **Fig. S5**. The surface of the original simple physical mixing system UF+MKP/0 contains a large number of irregularly shaped MKP blocks, and the EDX results also indicate that they are MKP, which should be due to poor compatibility between the two

components, leading to the aggregation of inorganic particles MKP on the surface of the UF matrix. Unlike UF+MKP/0, the original UF/MKP/0 surface deposits many needle-shaped MKP crystals with a diameter of about 80 nm, consistent in size and morphology. The EDX test results also exhibit that the two components are uniformly distributed in the nano fertilizer. After 10 days of soil cultivation, on the surface of UF+MKP/10, the MKP blocks disappear entirely, and the smooth UF surface is exposed. The EDX test results also display that the fertilizer contains almost no MKP. For UF/MKP/10, the EDX results show that it also contains a certain amount of MKP, and its SEM photographs display that the dissolved and released MKP produced many micropores, making the fertilizer surface very rough. The average pore size of these micropores obtained by testing is about 500 nm, about 10 times that of UF/MKP/0, leading to a sharp increase in the degradation sites of enzymes and water. At 40 days, only partial cracks and pores appear on the smooth UF surface in the simple physical mixing system. UF matrix in the hydrogen bonding system has been seriously eroded, with many pores of varying sizes on its surface. Its EDX test results show that the fertilizer also contains a small amount of MKP. After 70 days, the overall appearance of UF+MKP/70 remains well, with only some tiny eroded areas appearing on its surfaces, indicating that the system is challenging to hydrolyze or degrade by microorganisms in a short period. Unlike UF+MKP/70, there are many large cracks, irregular blocks, and deep holes on the surface of UF/MKP/70. In addition, many spherical-shaped degrading bacteria tightly adhere to its surfaces, as shown by the red arrows, indicating that UF/MKP is strongly attacked by microorganisms and that the nanocomposite can provide a suitable environment for microbial colonization. At 100 days, the overall appearance of UF+MKP/100 is still not significantly damaged, while the integrity of UF/MKP/100 no longer exists and becomes many adhesive fragments. The changes of the micromorphology and surface element contents of these two composites during the degradation process exhibit that the hydrogen-bond interaction between MKP and UF molecule in UF/MKP has a significant impact on degradation behavior of the polymer matrix UF and the release characteristic of the inorganic nanoparticle MKP.

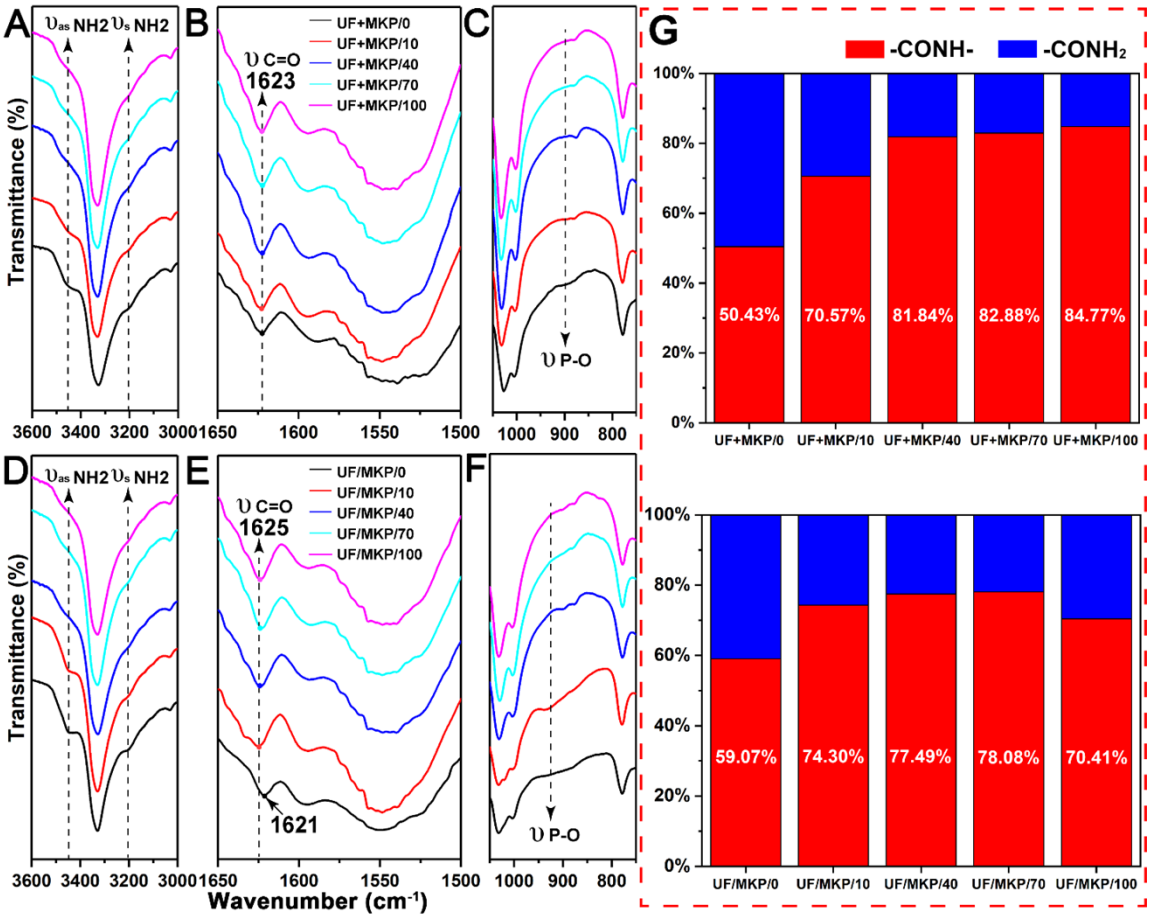

Fig. S6. FTIR spectrum of UF+MKP and UF/MKP at different soil culture periods in the regions of 3000-3600 cm^{-1} (A, D), 1500-1650 cm^{-1} (B, E), and 750-1050 cm^{-1} (C, F). (G) Relative content of different organic functional groups of UF+MKP and UF/MKP at different soil culture periods in the range 3050-3600 cm^{-1} in FTIR spectra quantified using a mixed Lorentzian-Gaussian function.

FTIR spectra were conducted to investigate further the molecular structure changes of UF+MKP and UF/MKP during soil degradation. As shown in **Fig. S6A** and **S6D**, the absorption bands at 3410-3456 cm^{-1} and 3200-3240 cm^{-1} could be assigned to the -NH_2 stretching vibration of the terminal group -$CONH_2$ in UF+MKP and UF/MKP. As degradation progresses, the intensity of these peaks decreases significantly, indicating that the terminal group -$CONH_2$ in both fertilizer systems is prone to degradation. In **Fig. S6C and S6F**, 840-960 cm^{-1} should be attributed to the P-O stretching vibration absorption peak in MKP, which completely disappears in UF+MKP/10, slightly decreases in UF/MKP/10, and only wholly disappears in

UF/MKP/40, indicating that the hydrogen-bonding interaction between inorganic particle MKP and polymer matrix UF can endow MKP, which is highly soluble in water, with excellent slow-release performance, consistent with the EDX results in **Fig. S5**. In **Fig. S6B**, the peak located at 1623 cm^{-1} is assigned to the stretching vibration of C=O, which remains at the same position during UF+MKP degradation. However, compared to UF/MKP/0, a distinct blue shift of the C=O stretching band in UF/MKP/10 is observed, as shown in **Fig. S6E**, clearly indicating that the hydrogen-bonding interaction between MKP and UF in UF/MKP gradually weakens with the release of MKP. Further, the FTIR spectra in the stretching vibration region of amide groups (3050-3600 cm^{-1}) of UF+MKP and UF/MKP were curve-fitted using a mixed Lorentzian-Gaussian function. The semi-quantitative distribution of amide groups determined by the fitting curve integral area is shown in **Fig. S6G**. The relative content of -CONH- in UF/MKP/0 increases by 8.64% compared with that in UF+MKP/0, indicating that the addition of MKP during the reaction process could indeed enhance the polymerization degree of the matrix UF and thus lead to a decrease in the relative content of its end-group -$CONH_2$. In the first 70 days, the relative content of -CONH- in the matrix UF of UF+MKP and UF/MKP has all been increasing. However, the relative contents of -CONH- in UF+MKP/10, UF+MKP/40, and UF+MKP/70 increase by about 40%, 62%, and 64%, respectively, compared to UF+MKP/0. While the relative contents of -CONH- in UF/MKP/10, UF/MKP/40, and UF/MKP/70 increase by about 26%, 31%, and 32%, respectively, compared to UF/MKP/0. On the one hand, the degradation of UF in the physical mixing system mainly occurs in its terminal group -$CONH_2$, that is, the chain-end degradation is dominant. On the other hand, the degradation rate of the non-terminal group -CONH- in the UF/MKP chains is much higher than that of UF+MKP. After 70 days, the relative content of -CONH- in UF+MKP still increases, with a 2% increase in UF+MKP/100 compared to UF+MKP/70. However, the relative content of -CONH- in UF/MKP decreases, with UF/MKP/100 decreasing by nearly 10% compared to UF/MKP/70. These indicate that the degradation rate of -CONH- in UF/MKP is significantly accelerated for 70 days, and further indicate that the -CONH- group in

UF/MKP is more easily degraded than that in UF+MKP. Therefore, the introduction of MKP, which can form intermolecular hydrogen bonds with UF, could result in a significant change of the degradation type of UF from typical chain-end degradation to the coexistence of chain-end degradation and random in-chain degradation.

Based on the above analysis results, the possible degradation and slow-release mechanisms of UF+MKP and UF/MKP in soil are proposed. For the simple physical mixing system UF+MKP, the degradation and release processes of its two components are essentially the same as those of the pure UF and the pure MKP, with little affecting each other only due to mixing at the macroscale. Specifically, for the component MKP, owing to its easily soluble nature in water, when the composite is applied to soil, all MKP particles quickly dissolve and diffuse into the soil solution. For the component UF, like the pure UF, degradation only occurs in its amorphous region and mainly takes place at the end of its macromolecular chain. Therefore, its degradation rate in the soil is prolonged, and the matrix is still firmly bound together after 100 days of cultivation in the soil. In contrast, for the hydrogen-bonding system UF/MKP, on the one hand, the increase in acidity of the reaction system caused by MKP leads to a higher polymerization degree of component UF. On the other hand, the macromolecular chains of UF are combined with a large number of MKP nanoparticles through hydrogen bonding, leading to an increase in the cross-linking degree of the UF molecular chains, further affecting the degradation and slow-release processes of UF and MKP, resulting in a significant difference from UF+MKP. Specifically, for the component MKP, when the nanocomposite is applied to soil, due to its hydrogen-bonding interaction with the matrix UF and the significant physical barrier of the UF macromolecular chains caused by mesoscopic dispersion, only a part of MKP particles dissolve in soil solution and then diffuse to the outside of the UF/MKP nanocomposite, which is particularly favorable for slow release of the elements contained in the composite, such as the elements P and K in this study. For the component UF, the increases in its polymerization degree and cross-linking degree lead to a lower initial degradation rate compared with the pure UF, and the hydrogen-bonding interaction between UF and MKP leads to a decrease in the ordered

arrangement of its molecular chains, which also enables the mixing of these two components at a mesoscale, resulting in significantly better activity, adsorption performance, and contact area with water and microorganisms of the UF macromolecular chains compared to macroscopic mixed material systems, namely simple physical mixtures. Especially the large number of micropores left in the system after the release of nano-MKP particles, compared to the macroscale mixed system UF+MKP, not only have a more significant number but also evenly spread throughout the entire material system, increasing the contact area between UF molecular chains and water and microorganisms, thereby significantly improving the degradation rate of matrix UF at the initial stage of cultivation, and further changing its degradation type from chain-end scission of the pure UF to coexist of the chain-end scission and the random chain cleavage. Obviously, this is of great help in improving the element release rate of high crystallinity matrix, such as element N in UF in this study.

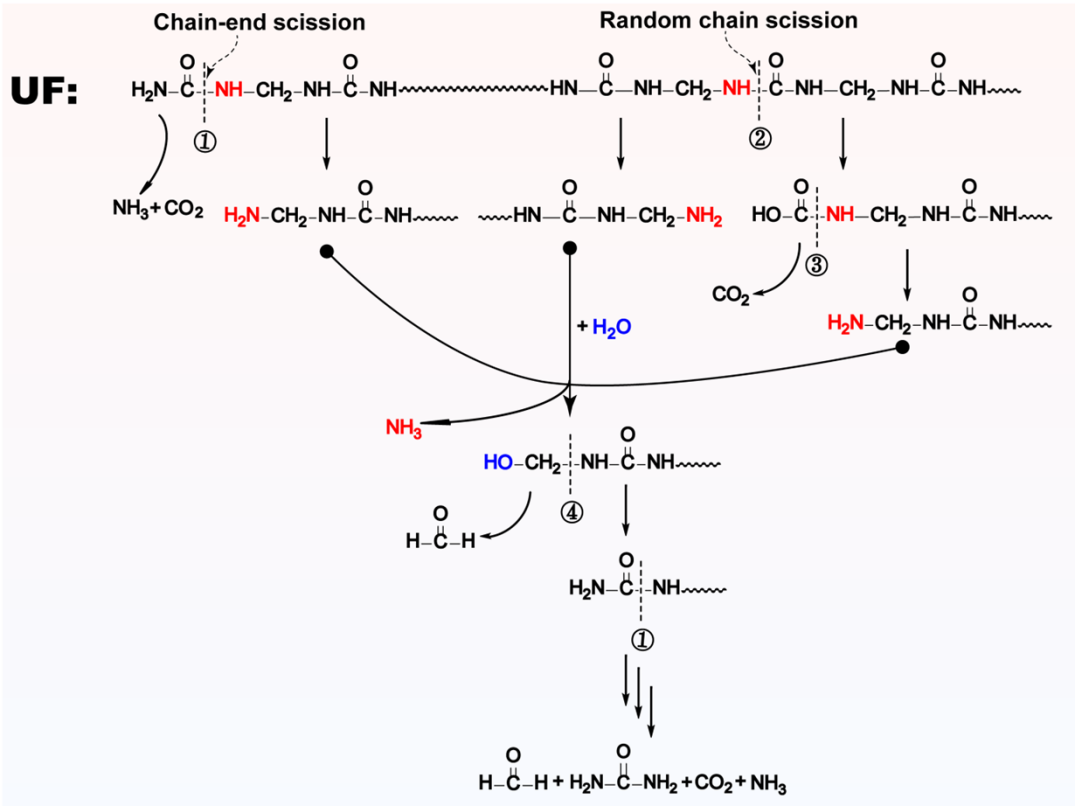

Fig. S7. The detailed chain-scission mechanism of UF matrix at molecular level.

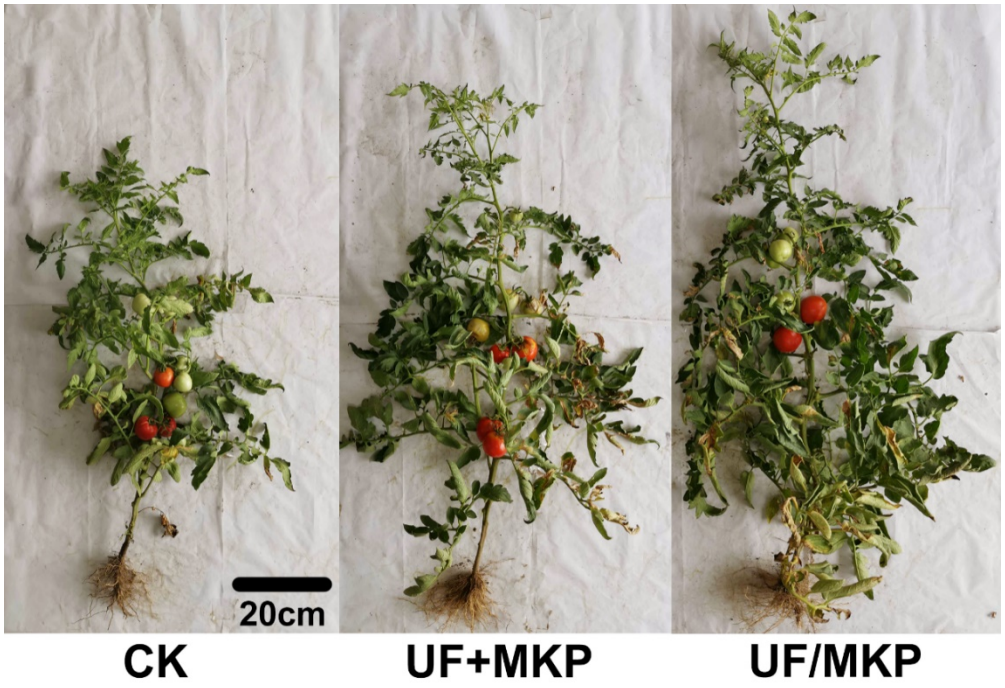

Fig. S8. Images of representative plants on day 100 in different composite treatments.